Electronic Supplementary Material (ESI) for Nanoscale.
This journal is © The Royal Society of Chemistry 2020

Electronic Supplementary Information

Encapsulation of Fe nanoparticles into N-doped carbon nanotubes/nanosheets integrated hierarchical architecture as an efficient and ultrastable electrocatalyst for oxygen reduction reaction

Xiaoge Li[a], Lu Ni[a], Jinhua Zhou[a], Lin Xu[b] *, Chunliang Lu[c], Gaixiu Yang[d], Weiping Ding[a], Wenhua Hou[a] *

[a] *Key Laboratory of Mesoscopic Chemistry of MOE, School of Chemistry and Chemical Engineering, Nanjing University, Nanjing, 210023, P. R. China*

[b] *Jiangsu Key Laboratory of New Power Batteries, Jiangsu Collaborative Innovation Center of Biomedical Functional Materials, School of Chemistry and Materials Science, Nanjing Normal University, Nanjing, 210023, P. R. China*

[c] *Analytical Testing Center, Yangzhou University, Yangzhou, 225009, P. R. China*

[d] *Key Laboratory of Renewable Energy, Chinese Academy of Sciences, Guangzhou Institute of Energy Conversion, Chinese Academy of Sciences, Guangzhou 510640, P. R. China*

* Corresponding author.

E-mail addresses: whou@nju.edu.cn (W. Hou); xulin001@njnu.edu.cn (L. Xu)

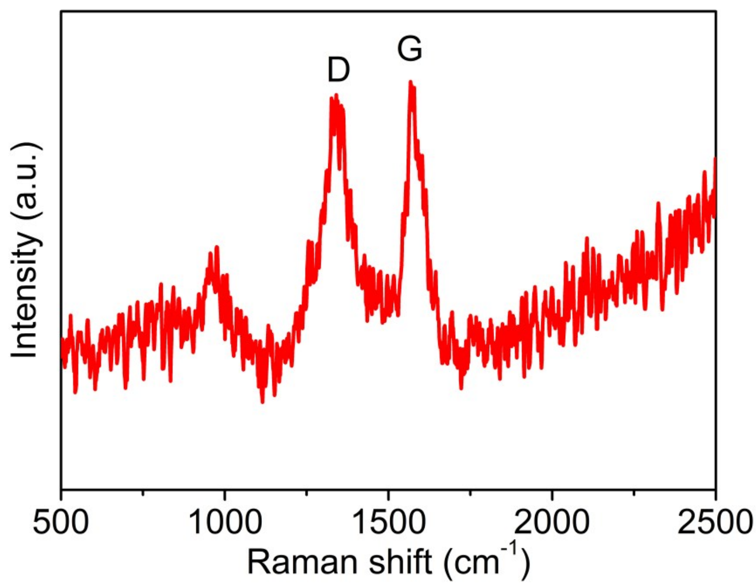

Fig. S1 Raman spectrum of Fe@N-C NT/NSs.

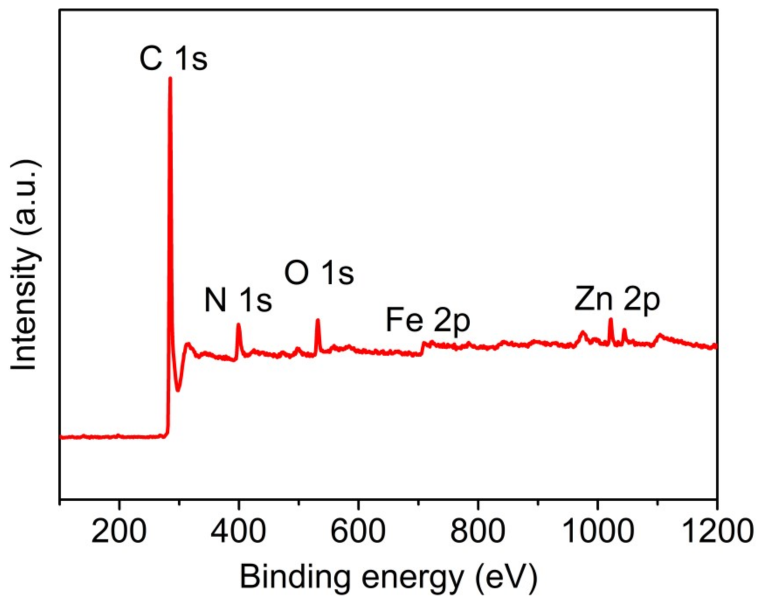

Fig. S2 XPS survey spectrum of Fe@N-C NT/NSs.

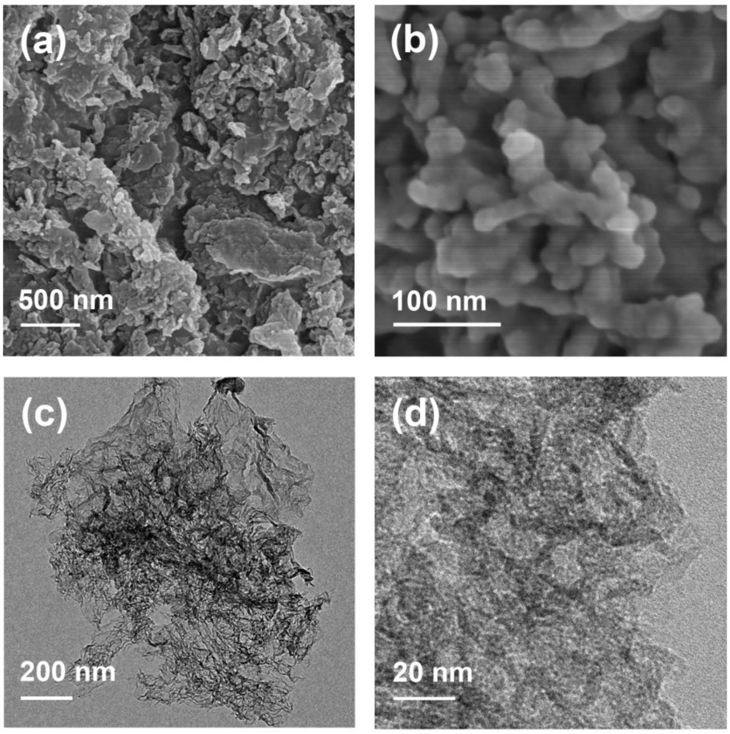

Fig. S3 SEM (a, b) and TEM (c, d) images of N-C.

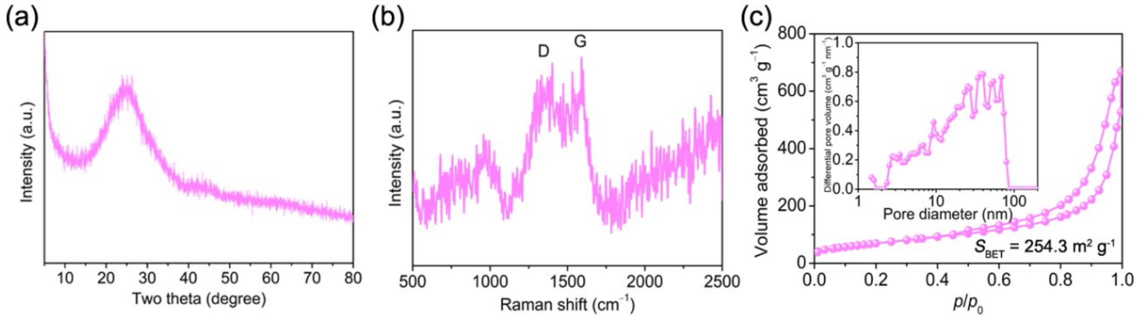

Fig. S4 (a) XRD pattern, (b) Raman spectrum and (c) N_2 adsorption-desorption isotherms (inset is the corresponding pore-size distribution curve) of N-C.

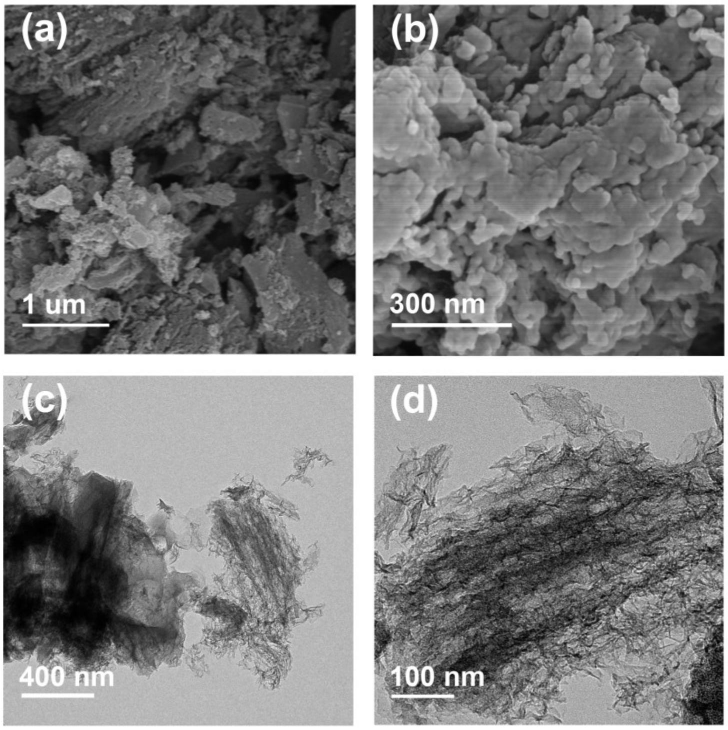

Fig. S5 SEM (a, b) and TEM (c, d) images of N-C'.

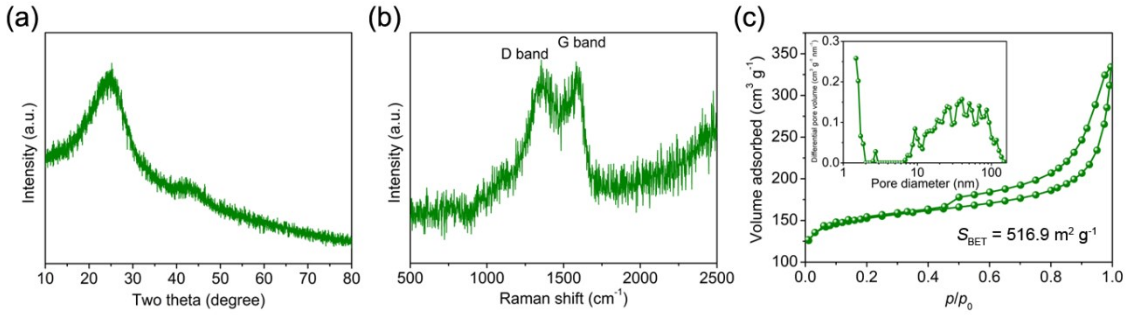

Fig. S6 (a) XRD pattern, (b) Raman spectrum and (c) N_2 adsorption-desorption isotherms (inset is the corresponding pore-size distribution curve) of N-C'.

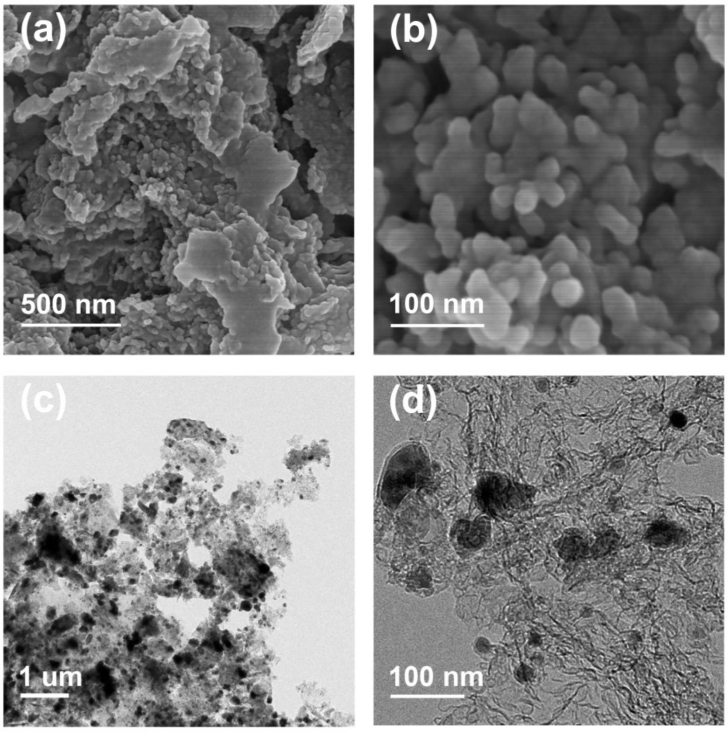

Fig. S7 SEM (a, b) and TEM (c, d) images of Fe@N-C NSs.

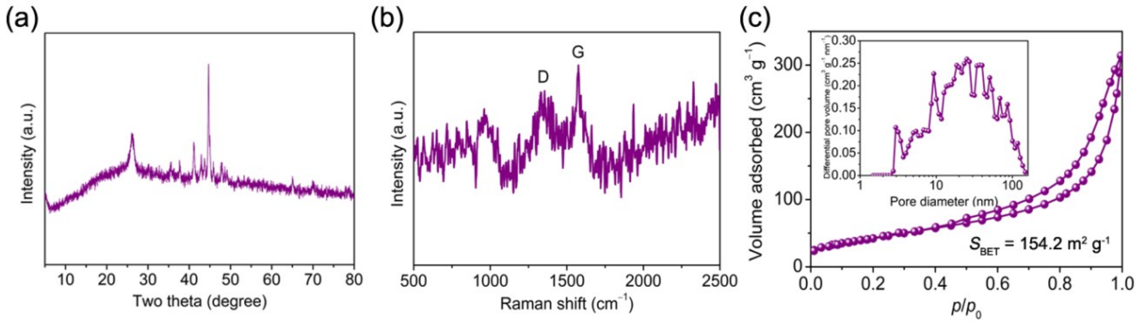

Fig. S8 (a) XRD pattern, (b) Raman spectrum and (c) N_2 adsorption-desorption isotherms (inset is the corresponding pore-size distribution curve) of Fe@N-C NSs.

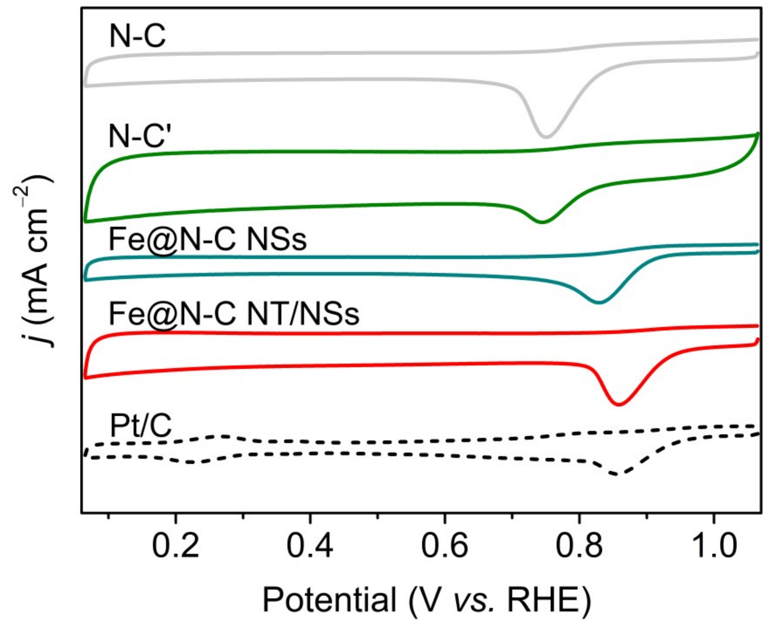

Fig. S9 CV tests of N-C, N-C', Fe@N-C NSs, Fe@N-C NT/NSs and Pt/C for ORR in O_2-saturated 0.1 M KOH solution at a scan rate of 10 mV s^{-1}.

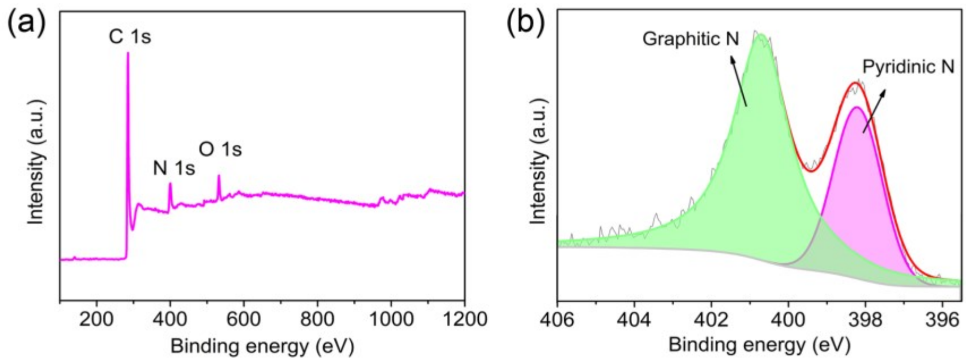

Fig. S10 (a) XPS survey spectrum and (b) N 1s XPS spectrum of N-C.

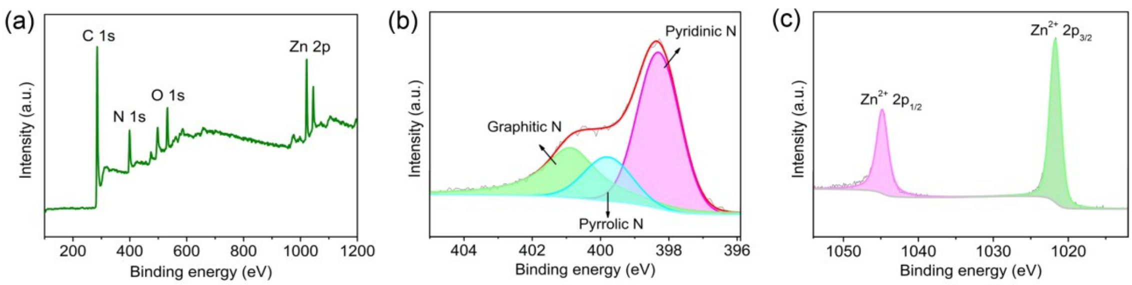

Fig. S11 (a) XPS survey spectrum, (b) N 1s XPS spectrum, (c) Zn 2p XPS spectrum of N-C'.

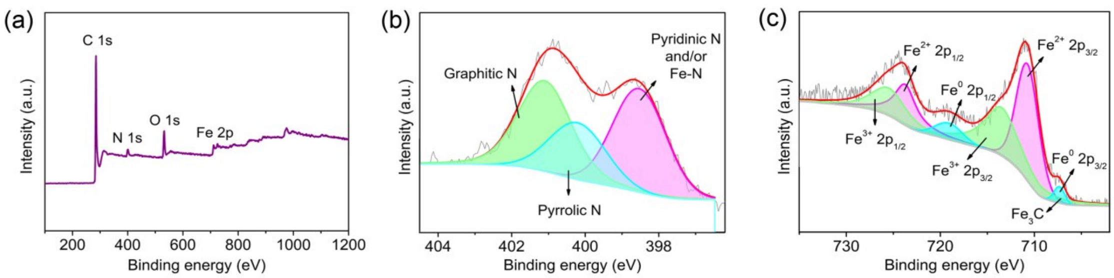

Fig. S12 (a) XPS survey spectrum, (b) N 1s XPS spectrum, (c) Fe 2p XPS spectrum of Fe@N-C NSs.

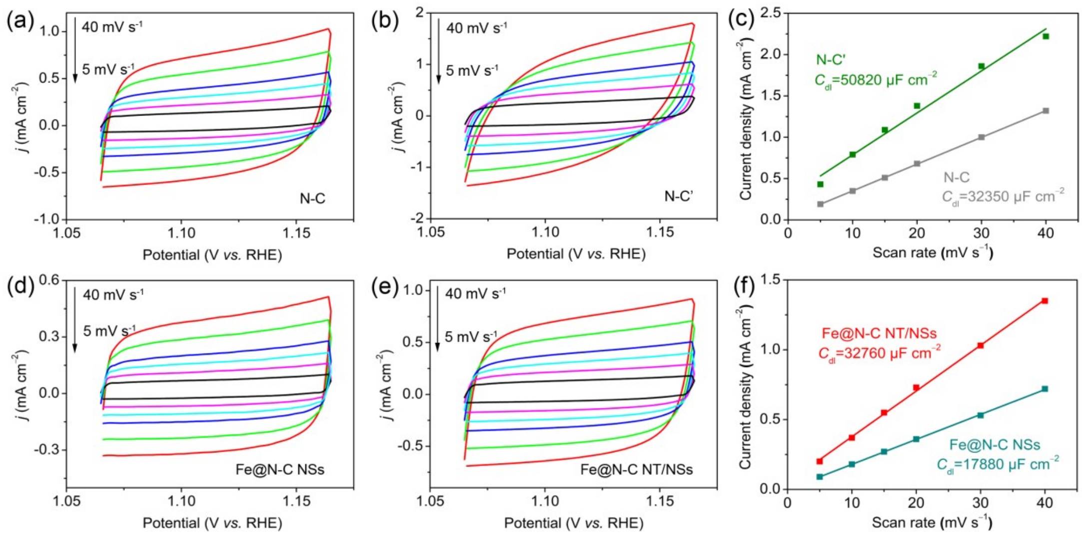

Fig. S13 CV curves of (a) N-C, (b) N-C', (d) Fe@N-C NSs and (e) Fe@N-C NT/NSs at scan rates of 5, 10, 15, 20, 30 and 40 mV s^{-1}, (c) and (f) current density (taken at the potential of 1.115 V) as a function of scan rate derived from (a), (b), (d) and (e).

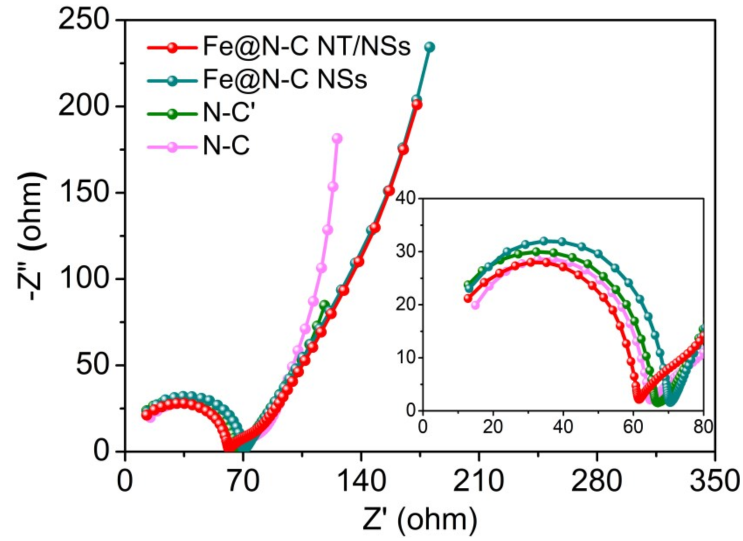

Fig. S14 Nyquist impedance plots of N-C, N-C', Fe@N-C NSs and Fe@N-C NT/NSs.

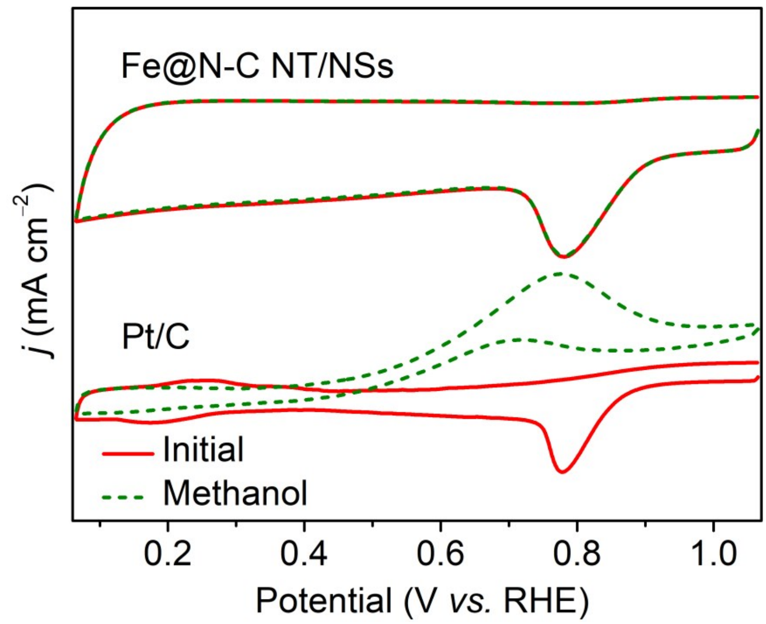

Fig. S15 CV curves at a scan rate of 50 mV s^{-1} before and after the injection of 1 mL of methanol into 100 mL of O_2-saturated 0.1 M KOH solution.

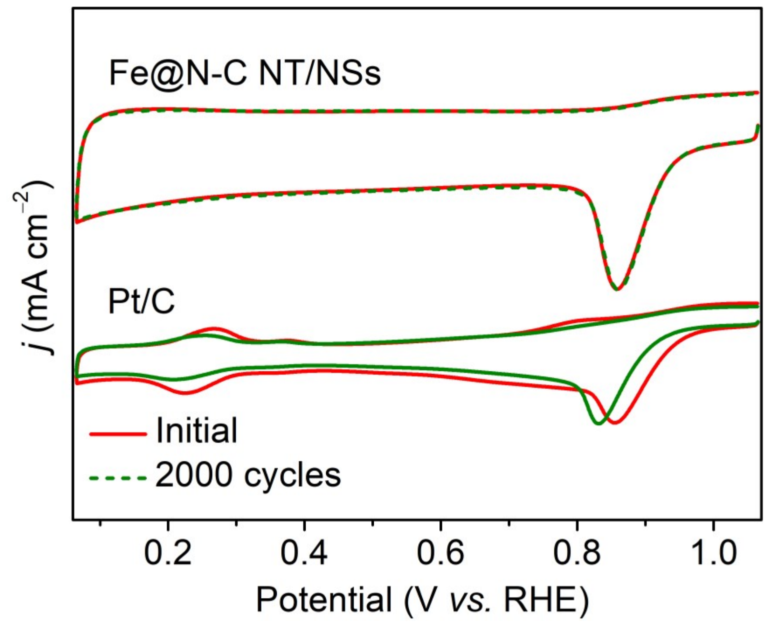

Fig. S16 CV curves of Fe@N-C NSs and Pt/C before and after 2000 cycles in O_2-saturated 0.1 M KOH solution at a scan rate of 10 mV s^{-1}.

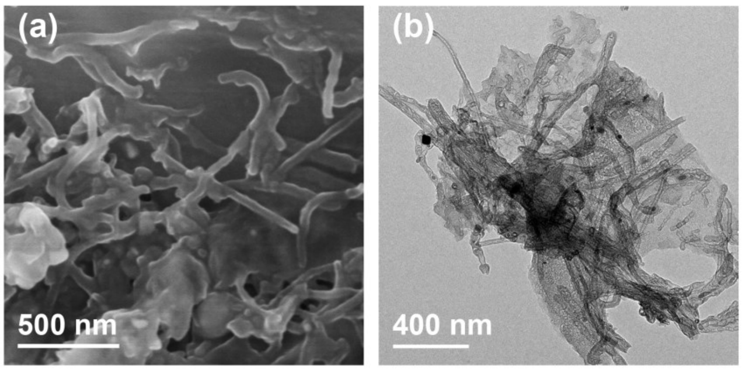

Fig. S17 (a) SEM and (b) TEM images of Fe@N-C NT/NSs after the long-term stability test for 96 h.

Table S1 Comparison of electrochemical ORR performance of Fe@N-C NT/NSs with the representative transition-metal-based catalysts reported in literatures (electrolyte is 0.1 M KOH).

Sample	E_{onset}[a]/V	$E_{1/2}$[b]/V	j[c]/mA cm^{-2}	**Ref.**
Fe@N-C NT/NSs	1.0	0.82	7.3	this work
CeO_2−Co−NC	0.92	0.80	5.37	*ACS Nano* **2018,** 12, 3042-3051
Fe_3C/C-800	1.05	0.83	~3.8	*Angew. Chem. Int. Ed.* **2014,** 53, 3675-3679
Co-CNTFs	~0.87	~0.77	~5.2	*Energy Storage Mater.* **2018,** 11, 112-117
Fe_3C/b-NCNT	0.96	NA	~6.8	*Chem. Eur. J.* **2017,** 23, 12125-12130
Fe_3C@N-CNT	NA	0.85	6.0	*Energy Environ. Sci.* **2016,** 9 (10), 3092-3096
l-CCNTs-Co-800	0.90	0.84	5.0	*Angew. Chem. Int. Ed.* **2018,** 57, 13187-13191
Cu_3P@NPPC-650	NA	0.78	~5.5	*Adv. Mater.* **2017**, 1703711
C-MOF-C2-900	NA	0.82	6.0	*Adv. Mater.* **2018**, 1705431
Cu-N/C	0.91	0.81	5.5	*Small* **2017,** 13, 1700740
Co/Co-N-C	0.82	NA	~3.2	*Adv. Mater.* **2019**, e1901666
N-Co_3O_4@NC-2	0.89	0.77	5.9	*Adv. Funct. Mater.* **2019**, 1902875
Co-Cat-T550	0.96	0.86	5.2	*ACS Appl. Mater. Interfaces* **2020**, DOI: 10.1021/acsami.0c02884
CoSAs/PTF-600	NA	0.81	6.1	*J. Mater. Chem. A* **2019**, 7, 1252–1259
NdC-CoNPs-NdC-700	NA	0.80	6.0	*Nanoscale* **2020**, DOI: 10.1039/C9NR09779A
Co-Fe-P-Se/NC	NA	0.76	4.0	*Nanoscale* **2019,** 11, 20144-20150
Fe-N-CPNS	NA	0.84	5.8	*Nanoscale* **2020,** 12, 5601-5611
CoPNi-N/C	0.93	0.84	~4.5	*Appl. Catal. B Environ.* **2019**, 240, 112–121
Co-GO(50)-C/N(2.5)	0.93	0.83	~5.2	*J. Power Sources* **2019**, 425, 76–86
MgO@Phen-Fe-800-3/1	0.94	0.80	~6.5	*J. Power Sources* **2019***,* 431, 31–39
Fe_3C@NG	0.99	NA	5.5	*ACS Appl. Mater. Interfaces* **2015**, 7, 21511-21520
200-CNTs-Co/NC	0.96	0.84	~5.4	*Chem. Eur. J.* **2018**, 342, 163-170

[a] Onset potential (*vs.* RHE). [b] Half-wave potential (*vs.* RHE). [c] Diffusion-limited current.